Journal of Health and Environmental Research
2023; 9(2): 67-75
http://www.sciencepublishinggroup.com/j/jher
doi: 10.11648/j.jher.20230902.14
ISSN: 2472-3584 (Print); ISSN: 2472-3592 (Online)

Land Surface Temperature and Thermal Radiation Estimate from Remote Sensed Data: Implications for Human Health in Owo, Ondo State, Nigeria

Oluwadare Ayoola Olamitomi[1, *], Oluwadare Esolomo John[2], Olofin Emmanuel Oluwafemi[3]

[1]Department of Physical and Chemical Sciences, Elizade University, Ilara Mokin, Nigeria

[2]Department of Physics, Ajayi Crowther University, Oyo, Nigeria

[3]Department of Water Resources Management and Agro-Meteorology, Federal University, Oye Ekiti, Nigeria

Email address:

ayoola.oluwadare@elizadeuniversity.edu.ng (Oluwadare Ayoola Olamitomi)

[*]Corresponding author

To cite this article:

Oluwadare Ayoola Olamitomi, Oluwadare Esolomo John, Olofin Emmanuel Oluwafemi. Land Surface Temperature and Thermal Radiation Estimate from Remote Sensed Data: Implications for Human Health in Owo, Ondo State, Nigeria. *Journal of Health and Environmental Research.* Vol. 9, No. 2, 2023, pp. 67-75. doi: 10.11648/j.jher.20230902.14

Received: May 8, 2023; **Accepted**: May 30, 2023; **Published**: June 15, 2023

Abstract: The use of remote sensing data to study the spatial distribution of land surface temperature (LST) and thermal radiation has revealed the negative impact of urban heat islands on human health. As an increase in LST and thermal radiation can have serious health consequences, it is important to constantly evaluate and gather information on the extent of these changes in a given region. Such information is crucial for public health and environmental epidemiology, as it enables emergency response planners and public health specialists to identify the areas most at risk and use scientific findings to improve the health of the affected populations. Remote sensing data from the Landsat Thematic Mapper (LANDSAT 7) image of 2002 and the Operational Land Imager and Thermal Infrared Sensor (LANDSAT 8) images of 2014 and 2018 were utilized to estimate the spatial distribution of land surface temperature and thermal radiation in Owo, Ondo State, Nigeria. The study found that the rapid urbanization and modification of the vegetation cover and natural surfaces in Owo had contributed to an increase in land surface temperature and thermal radiation. The research also noted that areas with low vegetation cover had higher surface temperatures, while areas with high vegetation cover had lower surface temperatures. Additionally, the study found that areas with higher surface temperatures were associated with increased thermal radiation, following a similar pattern to that of the spatial distribution of land surface temperature. In particular, regions with higher land surface temperatures emitted more thermal radiation compared to regions with lower land surface temperatures. The results of this study can provide valuable insights for the public health department of Ondo State in terms of understanding, managing, and taking action to improve the health and well-being of residents, particularly those residing in areas that are most impacted by the urban heat island effect.

Keywords: Land Surface Temperature, Thermal Radiation, Remote Sensing, Human Health

1. Introduction

The escalating temperature in urban areas is a significant issue in many developing countries, posing a threat to human health and existence. Urban areas typically have a higher absorption of solar radiation, greater thermal capacity, and conductivity, resulting in heat storage during the day and release at night. Consequently, urban areas experience higher temperatures than surrounding rural areas. This temperature difference, combined with heat emitted from urban houses, transportation, and industries, contributes to the development of the urban heat island (UHI) phenomenon. UHI is influenced by physical, human, and anthropogenic factors such as uncontrolled urbanization, reduction of natural resources and forest and agricultural land, changes in land use patterns, a heavy concentration of industries, an increasing vehicular population, and higher levels of energy consumption. These factors can alter local climate and weather parameters in the region [1-3]. The presence of vegetation in urban areas helps to

regulate temperatures and create cooler environments. However, human activities such as covering natural surfaces with asphalt, concrete, and buildings can alter vegetation cover and result in reduced evapotranspiration, increased surface temperatures, and rapid run-off, ultimately leading to the creation of UHI [4-5]. Land use and land cover changes also have significant impacts on local and regional climates, particularly on land surface temperature (LST) and thermal radiation, which tend to increase with changes in land cover, particularly in urban areas [6-7]. Due to the recognized risks of UHI on both human life and the environment, several studies have explored the health implications of rising land surface temperature and thermal radiation [7-9]. For instance, researchers found that mortality rates during heat waves in Shanghai increased significantly with higher temperatures, and UHI intensified this effect. Moreover, cities affected by UHI were found to be 5°C to 11°C warmer than surrounding rural areas [10]. These health concerns have been identified by various indicators, including the global solar radiation index threshold and the thermal comfort index, among others [11-14].

While it is possible to obtain meteorological measurements of air temperature and solar radiation parameters from airports or other weather stations, the number of observing stations that measure these parameters is limited. Additionally, ground-based monitoring and measuring techniques have limitations when it comes to capturing spatial variations of these parameters, especially over large areas. Therefore, there is a growing need to utilize remote sensing (RS) techniques, which have the potential to retrieve distributed estimates of these parameters at local, regional, and even global scales [15]. Remote sensing techniques are commonly employed to determine surface temperatures over large and diverse areas, monitor urban growth, and detect changes in land use and land cover that may lead to environmental issues in urban areas [6-9, 15-18]. Geospatial technologies are also providing valuable information for environmental epidemiology and public health through the use of land surface temperature data obtained from remote sensing. This emerging trend enables emergency response planners and public health practitioners to identify high-risk areas and utilize scientific outputs to reform policies and practices [6, 8-9, 19].

To address the increasing public health concern related to heat-related illnesses and deaths as a result of climate change, it is necessary to identify areas of high vulnerability to heat in cities. One approach is to predict these areas through the use of epidemiologic studies that employ satellite-derived temperatures and land cover data, rather than relying on temperature data from the nearest airport. This method has the potential to provide more accurate heat exposure classifications. In a Philadelphia study, remote sensing technique was employed to identify the spatial correlation between vulnerable populations, urban heat island intensities, and mortality during an extreme heat event [19].

Owo town and its neighbouring areas in Ondo State, Nigeria, are experiencing rapid urbanization, which is attracting a significant number of people and leading to a surge in demand for housing and commercial establishments. However, this surge in activity is putting strain on land resources in and around urban centres, resulting in constant changes in land use and impacting the local microclimate. To design effective strategies for mitigation and adaptation, it is important to monitor changes in land surface temperature and thermal radiation in Owo. Thus, this study aimed to estimate land surface thermal characteristics using high-resolution Landsat images, with a focus on surface land temperature and land surface solar radiation. By quantifying the spatial distribution of LST and thermal radiation in Owo, this study sought to provide valuable insights for designing appropriate mitigation and adaptation strategies.

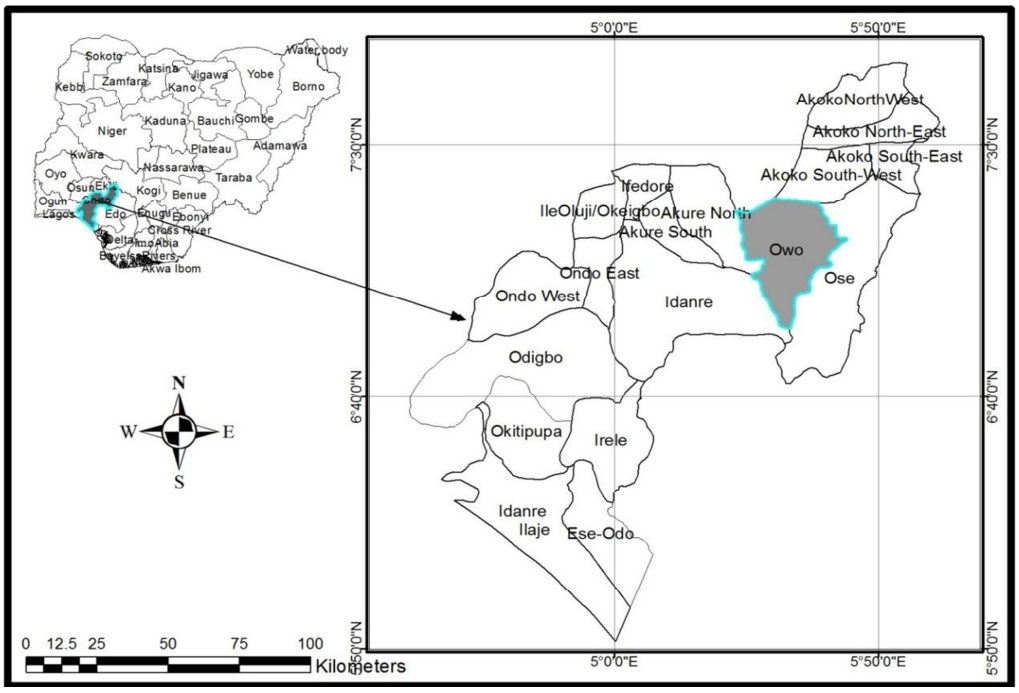

Figure 1. *Map of Nigeria showing Ondo State with Owo town. Source: Akeju et al [20].*

2. Study Area

Owo is a major town and one of the local government areas in Ondo State, Nigeria. It lies approximately at 7° 12′ North of the Equator and 5° 35′ East of the Greenwich Meridian, as shown in Figure 1. The temperature is relatively high throughout the year with an average daily temperature of about 27°C (80.6°F) and marked seasonal changes in rainfall and relative humidity. This region is characterized by a monsoon climate. Over the years, Owo City has experienced huge growth in the size of built-up areas, the number of immigrants, transportation, and commercial activities. The area had a population of 157,191 in 1991, 222,262 based on the 2006 population census [21], and was projected to have about 341,400. Currently, the city houses two higher education institutions (Rufus Giwa Polytechnic, Owo, and Achieves University, Owo) and a federal medical center.

3. Materials and Methods

3.1. DATA

Landsat satellite images of Owo town were acquired from the archives of the US Geological Survey (USGS). The images collected for the analysis were in three components: image data from 2002, 2014, and 2018, which were cloud-free in the selected area. The area of study is located in the path/row 190/55 of the Landsat images, these images were downloaded from http://glovis.usgs.gov.

Table 1. *Description of the satellite images used.*

Satellite Sensor	Spatial Resolution (m)	Acquisition date	Path/Row	Satellite overpass time
LandSat 7 ETM+	30/60	2002-01-03	190/055	09:45
Landsat 8 OLI_TIRS	30/100	2014-01-12	190/055	09:57
Landsat 8 OLI_TIRS	30/100	2018-01-07	190/055	09:56

Table 1 gives a detailed description of the satellite images used: satellite sensors, spatial resolutions, acquisition date, and satellite overpass time. The selection of images was done such that the period of assessment was the same (dry season in January) to ensure consistency in vegetation and land use change comparison. The Operational Land Imager (OLI) image comprises the Near-Infrared (NIR) band, Shortwave Infrared (SWIR) band, Visible (RED) band, and Thermal Infrared (TIR) band, which are also present in the 2002 ETM+ image.

3.2. Data Processing

3.2.1. Conversion of the Digital Number to Spectral Radiance

The spectral radiance of the Landsat 7 data was computed from the digital number (DN) following the technique presented by Chander and Markham [22].

$$L_\lambda = \left(\frac{LMAX_\lambda - LMIN_\lambda}{QCALMAX - QCALMIN} \right) \times (QCAL - QCALMIN) + LMIN_\lambda \quad (1)$$

where L_λ is the Top of Atmosphere (TOA) observed radiance [$Wm^{-2}ster^{-1}\mu m^{-1}$], $LMAX_\lambda$ [$Wm^{-2}ster^{-1}\mu m^{-1}$], and $LMIN_\lambda$ [$Wm^{-2}ster^{-1}\mu m^{-1}$] are the calibration constants, *DN* [-] is the digital number recorded in the satellite image, QCALMAX and QCALMIN are the highest and the lowest points of the range of rescaled radiance in DN and QCAL is the quantized and calibrated standard product pixel values (DN). While Landsat 8 data can be converted to TOA spectral radiance using the method described by USGS [23].

3.2.2. Calculation of NDVI

The normalized differential vegetation index (NDVI) for the study area was calculated as the ratio of the differences in reflectivity for the near-infrared (NIR) and visible (RED) portions of the electromagnetic spectrum to their sum.

$$NDVI = \frac{NIR - RED}{NIR + RED} \quad (2)$$

The NDVI is a sensitive indicator of the amount and condition of green vegetation. Values for NDVI range between -1 and +1. Green surfaces have an NDVI between 0 and 1. Water bodies usually have a negative value. NDVI was used for monitoring vegetation changes in the study area between 2002 and 2018.

3.2.3. Calculation of Land Surface Temperature

By first converting the spectral radiance of the thermal band of the three Landsat images to brightness temperature under the assumption of uniform emissivity, land surface temperature values in Kelvin were obtained.

$$T_b = \frac{K_2}{\ln\left(\frac{K_1}{L_\lambda} + 1\right)} \quad (3)$$

Where T_b is the brightness temperature, K_1 and K_2 are thermal constants found in the metadata associated with each Landsat data, and L_λ is the spectral radiance. The land surface temperature was then computed as the ratio of the brightness temperature to the surface emissivity [24].

$$T_s = \frac{T_b}{\varepsilon_0^{0.25}} \quad (4)$$

Where ε_0 is the surface emissivity, defined as the ratio of the energy flux emitted by the surface at a given temperature to that emitted by a black body at the same temperature and wavelength. The value of surface emissivity ranges from 0 to 1, and most earth's surface has an emissivity value between 0.95 and 0.99. ε_0 was estimated empirically following the relationship proposed by Bastiaanssen et al. and Tasumi et al. [25-26].

$$\varepsilon_0 = 1.009 + 0.047 \ln(NDVI) \quad (5)$$

The LSTs were converted into Celsius by subtracting 273.15 from the value obtained in Equation (4).

3.2.4. Estimation of Surface Radiation

The outgoing longwave radiation also referred to as "thermal radiation", depends on the emitting body's temperature. The radiant energy emitted by a body at a given temperature is explained by the Stefan-Boltzmann law; this outgoing longwave radiation was calculated by implementing the approach outlined by Bastiaanssen et al. [25].

$$R_{L\uparrow} = \varepsilon_0 \sigma T_s^4 \quad (6)$$

Where, σ is the Stefan-Boltzmann constant (5.670373×10^{-8} $Wm^{-2}K^{-4}$).

4. Result

4.1. Spatial Distribution of Normalized Difference Vegetation Index of Owo

The NDVI scale ranges from -1 to 1, where higher values indicate denser and healthier vegetation. Values near zero (between 0 and 0.2) typically indicate barren areas of rock, sand, soil, or man-made materials, while low positive values (0.2–0.4) represent shrub and grassland, and high values correspond to temperate and tropical rain forests, with NDVI values approaching 1. Water bodies generally have negative NDVI values. Figure 2 depicts the NDVI image of Owo for the years 2002, 2014, and 2018. The map's spatial distribution of red color represents areas with lower NDVI values, indicating less or no vegetation, while green areas indicate healthier vegetation and higher NDVI values.

4.2. Spatial Distribution of Land Surface Temperature in Owo, Ondo State

Over the past 16 years, Owo metropolis has experienced significant changes in its land surface characteristics since the establishment of the two higher institutions. Figure 2 illustrates the spatial distribution of land surface temperature in Owo and its environs for the years 2002, 2014, and 2018. The analysis revealed that built-up regions had a higher LST than areas covered with vegetation and other land features. The dark brown colour in Figure 3 represents the hottest regions or surfaces, while the light or dark purple colour depicts the coolest regions. The hot regions are typical of land cover types such as urban and rural areas, as well as tarred and concrete surfaces, whereas the cool regions are typical of land cover types such as water bodies, tropical rain forests, and healthier vegetated areas. It is also noteworthy that areas with higher surface temperatures correspond to areas with low NDVI values, while areas with lower surface temperatures correspond to areas with high NDVI values. There has been a decrease in the areas with temperatures ranging between 22°C and 24°C, represented by white and light or dark purple colors, over the years. This suggests a significant change in land cover or land use type, which may be due to deforestation and changes in agricultural practices. Meanwhile, there has been an increase in areas with high temperatures between 32°C and 35°C, indicating urban development. Urbanization alters the land cover of the area by reducing vegetation cover, increasing impervious cover, and creating complex surfaces, leading to higher surface temperatures. The results indicate that there were variations in LST between 2002 and 2018, and the areas with the highest temperatures remained consistent over the years. The built-up area consistently exhibited the highest LST values compared to other land features with lower LST values. One notable feature of Owo town is the observed increase in the built-up area between 2002 and 2014, with a clustering of high-temperature regions ranging from 34°C to 36°C in a particular area of the town. In contrast to 2014, in 2018, the clustered built-up area in Owo had reduced, indicating that the residents had spread out to other areas of the town. This expansion led to an increase in the areas with temperature ranges between 32°C - 36°C, particularly in areas near the Rufus Giwa Polytechnic, where 80.5% of the students live in rented houses outside the campus, which suggests urban growth. Furthermore, Figure 2c shows a reduction in vegetation cover in the region. One can observe that the urban heat island effect becomes increasingly evident as land surface temperature rises from the outskirts of built-up areas towards the inner city, making Owo town warmer than its surrounding areas. This observation is consistent with previous research findings that suggest deforestation can alter the surface thermal signal characteristics of a region [27-29]. The urban heat island effect in Owo is also observable over the years. Several studies have shown that exposure to excessive heat can lead to heat-related illnesses and even death, especially among vulnerable populations such as the elderly, infants, and individuals with pre-existing medical conditions, which can be exacerbated by the urban heat island effect [30-33].

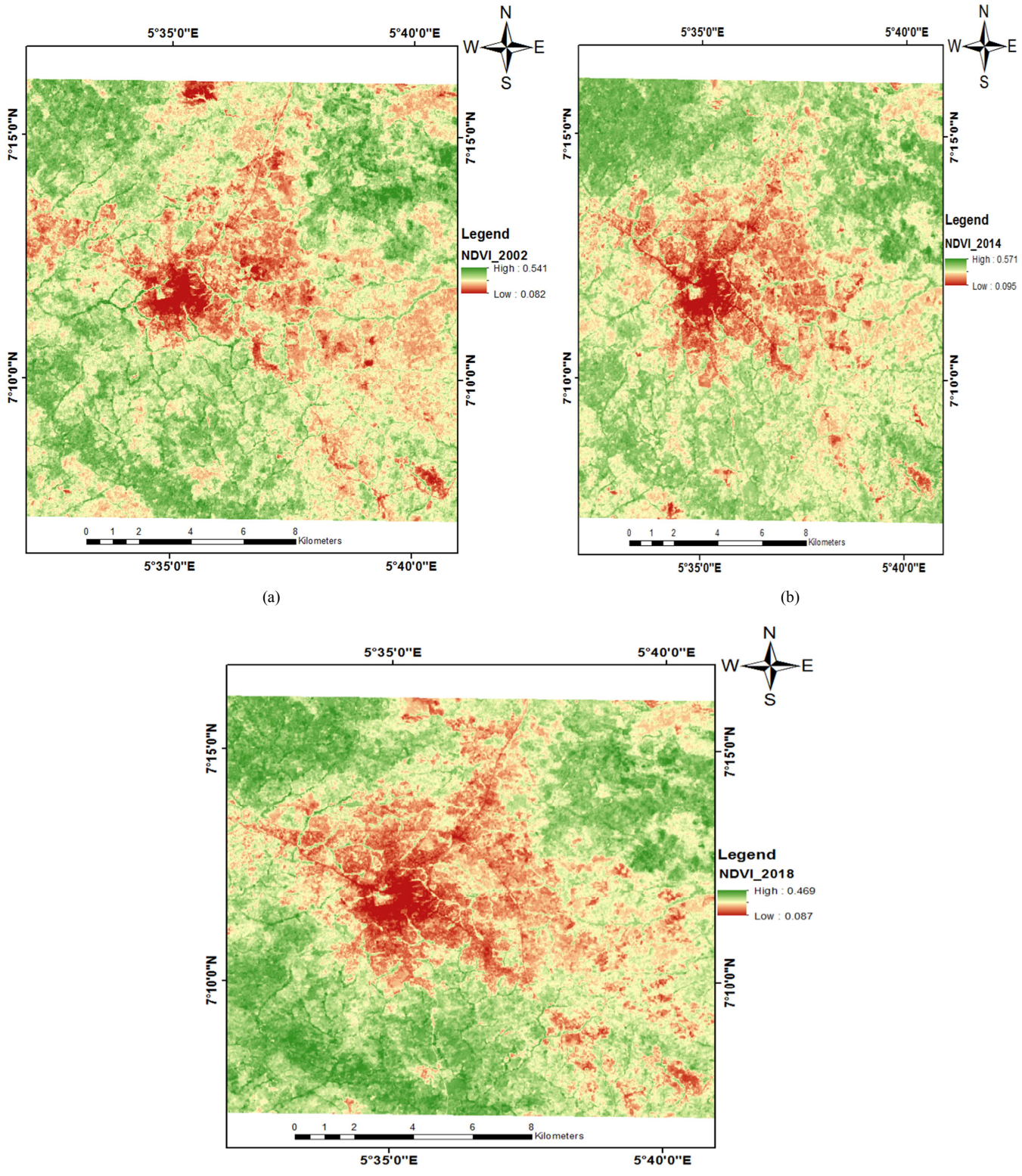

Figure 2. *Spatial distribution of NDVI of Owo and its Environ for 2002, 2014, and 2018.*

4.3. Spatial Distribution of Estimated Thermal Radiation and Its Impact on Human Health over Owo, Ondo State

After solar radiation from the sun reaches the Earth's surface, some of it is released as outgoing longwave radiation, also known as thermal radiation [34-35]. Figure 4 illustrates the spatial distribution of thermal radiation in Owo and its surrounding areas. The data showed that the spatial pattern of thermal radiation closely followed that of land surface temperature. In areas where land surface temperatures were

higher, more thermal radiation was emitted compared to areas with lower land surface temperatures.

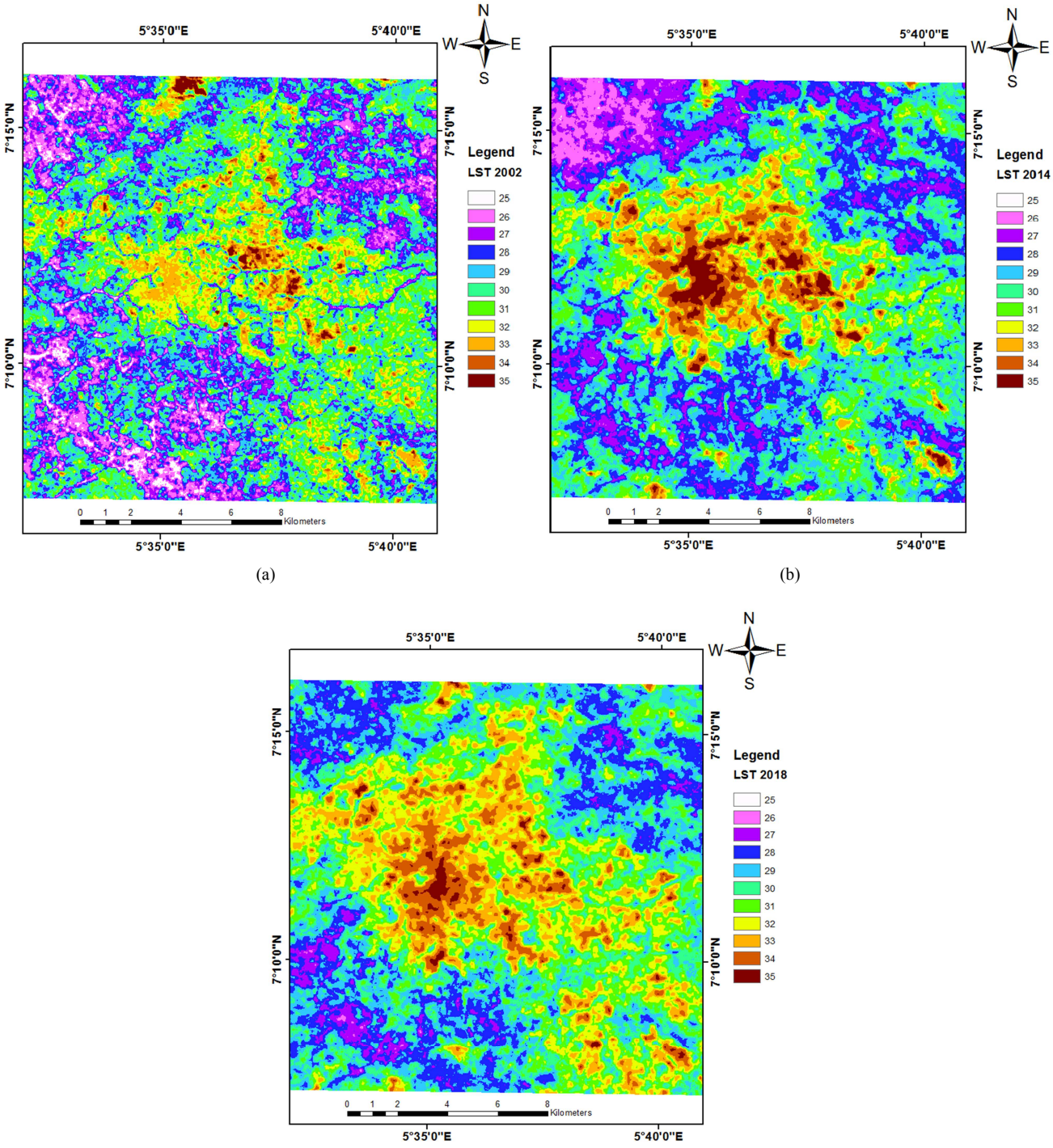

Figure 3. *Land Surface Temperature of Owo and its Environ for 2002, 2014, and 2018.*

Urban areas typically have rough and dry surfaces, as natural vegetation is replaced by impervious surfaces that reduce the amount of incoming solar radiation that can penetrate the surface. This leads to an increase in heat energy on the surface and the dissipation of thermal radiation into the surroundings. The results of the study indicate that there was a variation in thermal radiation between 2002 and 2018, with built-up areas and less vegetated areas emitting the highest thermal radiation levels consistently over the years, at greater than 460 Wm^{-2}. In 2002, 25.3% of the region had thermal radiation levels greater than 460 Wm^{-2}, while in 2014 and 2018, the percentages increased to 49.3% and 69.4%, respectively. The average thermal radiation for the region was 426.28 Wm^{-2}, 446.57 Wm-2, and 459.49 Wm^{-2} for the

years 2002, 2014, and 2018, respectively.

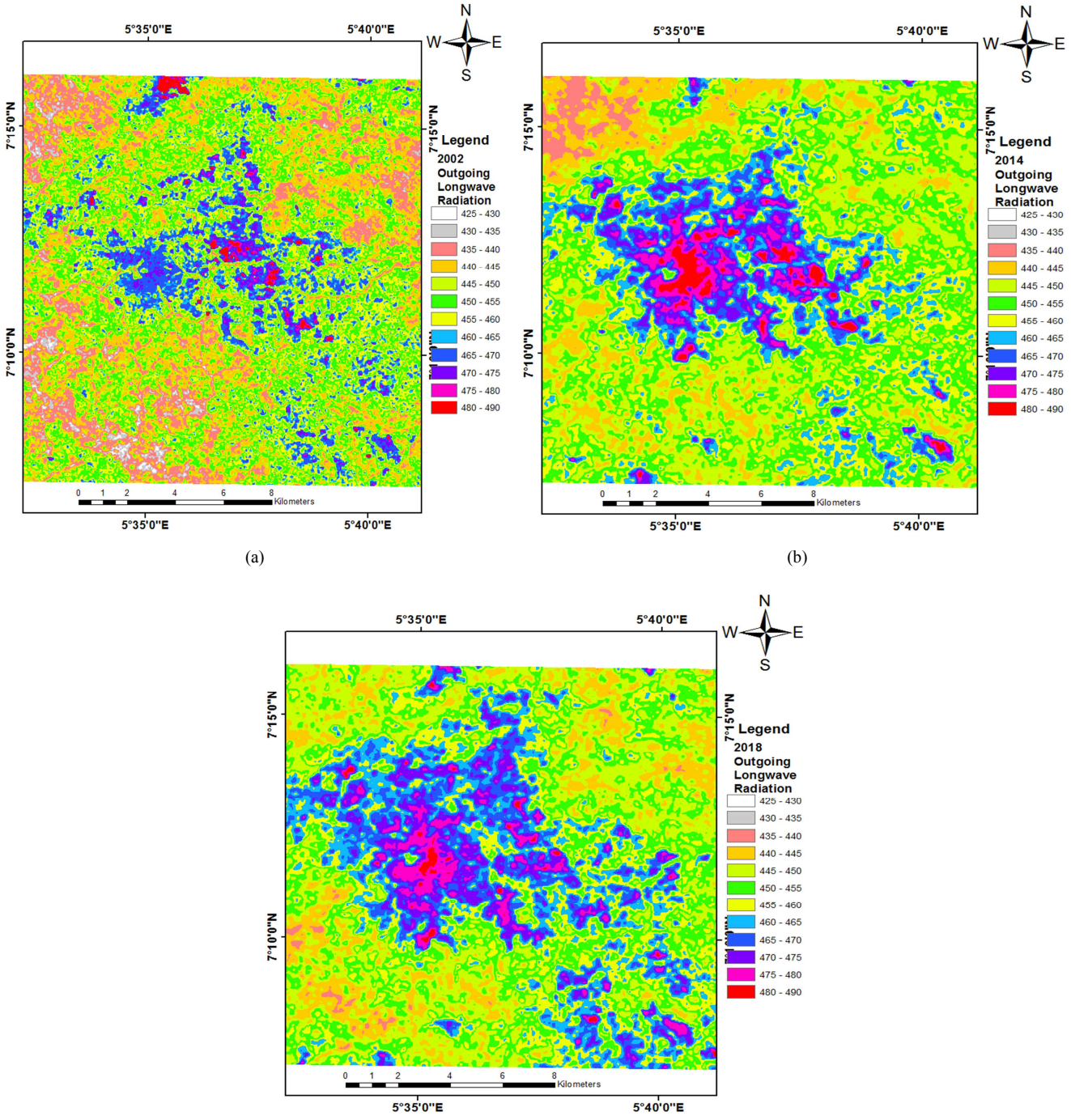

Figure 4. *Spatial distribution of estimated thermal radiation of Owo and its Environ for 2002, 2014, and 2018.*

As previously mentioned, when solar radiation reaches the Earth's surface, a portion of it is emitted as thermal radiation. However, many greenhouse gases, such as carbon dioxide (CO_2), water vapor, methane (CH_4), nitrous oxide (N_2O), and ozone (O_3), re-absorb this thermal radiation at specific wavelengths in the atmosphere. This results in the trapping of heat and prevents it from escaping into the upper atmosphere, leading to an increase in the Earth's surface temperature. Therefore, regions that emit higher levels of thermal radiation will have a greater amount of radiation trapped by these atmospheric gases, resulting in increased heat retention [36].

Although some of these greenhouse gases are naturally produced, in recent times, human activities such as fuel burning, deforestation, and changes in land use and agriculture have led to significant increases in the emission of these gases. While some of these gases have a shorter lifespan in the atmosphere (such as CH_4 and water vapor),

others like CO_2 and N_2O have a longer lifespan, leading to more significant radiation trapping. CH_4 and N_2O are particularly effective at trapping radiation compared to CO_2 [36-37]. With the continued increase in urban heat, there is a likelihood of an increase in the frequency and intensity of heat waves, as well as higher levels of air pollution. These conditions are expected to further exacerbate the already unhealthy living conditions in urban settlements, resulting in increased mortality rates [10].

Exposure to extreme heat has been linked to heat stroke, cardiovascular and respiratory diseases, and cerebrovascular diseases [33, 38]. Furthermore, populations living in the city centre are more vulnerable to the effects of excessive heat, as these areas tend to be hotter than surrounding areas [38]. Individuals who spend more time outdoors, such as outdoor workers, market women, and student-athletes, are particularly vulnerable to extreme heat exposure. Moreover, pregnant women, infants, the elderly, and people with certain medical conditions may also be at increased risk due to their reduced ability to regulate body temperature [33].

5. Conclusion

The investigation utilized remote sensing data to analyze the spatial distribution of land surface temperature and thermal radiation based on NDVI in the Owo Region of Ondo state from 2002 to 2018. The results revealed that urban development was a factor that contributed to the increase in both the magnitude and intensity of land surface temperature and thermal radiation.

Without interventions to increase vegetation in the urban area, continued urban development in Owo will lead to increased land surface temperatures and thermal radiation, exacerbating the negative impacts of climate change. These include higher temperatures, heat waves, and health threats to vulnerable populations such as children, pregnant women, and older adults. The findings of this study can help the public health department of Owo take action to improve the health and well-being of residents, especially those living in areas most affected by the changing climate. In addition, future research could explore the use of public health data to investigate the correlation between heat-related illnesses and meteorological conditions and to develop models that can predict the incidence of heat-related illnesses in the population in the coming years.

References

[1] Effat, H. A. and Hassan, O. A. K. (2014). Change detection of urban heat islands and some related parameters using multi-temporal Landsat images; a case study of Cairo city, Egypt. *Urban Climate*, 10: 171-188.

[2] Voogt, J. A. and Oke, T. R. (2003). Thermal remote sensing of urban climates. *Remote Sens Environ*, vol. 86, pp. 370–384.

[3] Akinbode, O. M., Eludoyin, A. O. and Fashae, O. A. (2008). Temperature and relative humidity distributions in a medium-size administrative town in southwest Nigeria. *Journal of Environmental Management*, 87: 95–105.

[4] Yue, W., Xu, J., Tan, W. and Xu, L. (2007). The relationship between land surface temperature and NDVI with remote sensing: Application to Shanghai Landsat 7 ETM+ data. *Int. J. Remote Sens*, vol. 28, pp. 3205–3226.

[5] Singh, R. B., Grover, A. and Zhan, J. (2014). Inter-Seasonal Variations of Surface Temperature in the Urbanized Environment of Delhi Using Landsat Thermal Data. *Energie*, vol. 7, pp. 1811–1828.

[6] Ige, S. O., Ajayi, V. O., Adeyeri, O. E. and Oyekan, K. S. (2017). Assessing remotely sensed temperature humidity index as human comfort indicator relative to landuse landcover change in Abuja, Nigeria. *Spat Inf Res*, 25 (4) 523–533.

[7] Weng, Q., Lu, D. and Schubring J. (2004). Estimation of land surface temperature-vegetation abundance relationship for urban heat island studies. *Remote Sens Environ*, 89 (4), 467–483.

[8] Orimoloye, I. R., Mazinyo, S. P., Nel, W. and Kalumba, A. M. (2018). Spatiotemporal monitoring of land surface temperature and estimated radiation using remote sensing: human health implications for East London South Africa. *Enviromental. Earth Sci*ences. 77 (3), 1-10.

[9] Oluwadare A. O., Oluwadare E. J. and Fagbemi S. (2019). Satellite Derived Estimate of Land Surface Temperature and Thermal Radiation: Human Health Implication for Akure, Ondo State, Nigeria. *Journal of the Nigerian Association of Mathematical Physics*. Vol. 50, pp. 303–310.

[10] Tan, T., Zheng, Y. and Tang, X. (2010). The urban heat island and its impact on heat waves and human health in Shanghai. *Int J Biometeorol* 54, 75–84.

[11] Tursilowati, L. and Djundjunan, J. D. (2007). Use of remote sensing and GIS to compute temperature humidity index as human comfort indicator relate with land use-land cover change (LULC) in Surabaya. Proceedings of the 73rd international symposium on sustainable Humanosphere, Bandung, Indonesia, pp. 160-166.

[12] Peng, S. S., Piao, S., Zeng, Z., Ciais, P., Zhou, L., Li, L. Z. and Zeng H. (2014). Afforestation in China cools local land surface temperature. *Proc Natl Acad Sci*, 111 (8), 2915–2919.

[13] Cheong, K. W. D., Djunaedy, E., Chua, Y. L., Tham, K. W., Sekhar, S. C. and Wong N. H. (2003). Thermal comfort study of an air-conditioned lecture theatre in the tropics. *Building and Environment*, 38 (1) 63–73.

[14] Xu, H., Hu, X., Guan, H. and He, G. (2017). Development of a fine-scale discomfort index map and its application in measuring living environments using remotely-sensed thermal infrared imagery. *Energy Build*, vol. 150, pp. 598–607.

[15] Oluwadare, A. O., Okogbue, E. C., Kunstmann, H., Akinluyi, F., Arnault, J., Tayari, S., Hingerl, L. and Bliefernicht J. (2018). Comparison of Sebal Estimated Heat Fluxes and Evapotranspiration using Field and Remote Sensing Data in the Sudanian Savanna in West Africa. International Journal of agriculture and Environmental Research, 4 (2) 352–374.

[16] Emmanuel Oluwafemi Olofin and Ayoola Olamitomi Oluwadare (2022). Settlement Growth and Its Impact on Land Surface Temperature in Ado-Ekiti, Ekiti State, Nigeria. *Frontiers*, 2 (2) Vol. 2, No. 2, pp. 88-97. doi: 10.11648/j.frontiers.20220202.12.

[17] Adeola, A. M., Botai, J. O., Rautenbach, C. D., Kalumba, A. M., Tsela, P. L. and Adisa O. M. (2017). Landsat satellite derived environmental metric for mapping mosquitoes breeding habitats in the Nkomazi municipality, Mpumalanga Province, South Africa. *South African Geographical Journal, Suid-Afrikaanse Geografiese Tydskrif*, 99 (1) 14–28.

[18] Eke, E. E., Oyinloye, M. A. and Olamiju, I. O. (2017). Analysis of the Urban Expansion for the Akure, Ondo State, Nigeria. *International Letters of Social and Humanistic Sciences,* vol. 75, pp. 41–55. doi: 10.18052/www.scipress.com/ILSHS.75.41.

[19] Johnson, D. P. and Wilson, J. S. (2009). The socio-spatial dynamics of extreme urban heat events: The case of heat-related deaths in Philadelphia. Appl Geogr, vol. 29, no. 3, pp. 419–434.

[20] Akeju Tolulope J., Oladehinde Gbenga J. and Abubakar Kasali (2018). An Analysis of Willingness to Pay (WTP) for Improved Water Supply in Owo Local Government, Ondo State, Nigeria. Asian Research Journal of Arts & Social Sciences, 5 (3): 1-15.

[21] National Population Commission (NPC), The 1991 and 2006 Population Census Reports.

[22] Chander, C. and Markham H. (2003). Revised Landsat-5 TM radio- metric calibration procedures and post-calibration dynamic ranges, *IEEE Trans Geosci Remote*, vol. 41, pp. 2674–2677.

[23] USGS. Using the USGS Landsat Level-1 Data Product. Accessed from https://www.usgs.gov/landsat-missions/using-usgs-landsat-level-1-data-product in May 2022

[24] Allen, R. G., Pereira, L. A., Raes, D. and Smith, M. (1998). *Crop evapotranspiration guidelines for computing crop water requirements*. FAO Irrigation and Drainage Paper No. 56, FAO, Rome.

[25] Bastiaanssen, W. G. M, Menenti, C., Feddes, R. A. and Holtslag, A. A. M. (1998). A remote sensing surface energy balance algorithm for land (SEBAL), Part I Formulation. *Journal of Hydrology*, vol. 212-213, pp. 198–212.

[26] Tasumi, M., Allen, R. G. and Bastiaanssen W. G. M. (2000). *The theoretical basis of SEBAL, Application of the SEBAL methodology for estimating consumptive use of water and stream flow depletion in the Bear River Basin of Idaho through remote sensing*. Raytheon Systems Company, Earth Observation System Data and Information System Project, pp. 46–69.

[27] Olofin, E. O. and Adebayo, W. O. (2017). *Effects of Deforestation on Land Degradation. Saarbrucken, Germany.* LAMBERT Academic Publishing, 63.

[28] Wang, C., Myint, S. W., Wang, Z. and Song J. (2016). Spatio-temporal modeling of the urban heat island in the Phoenix metropolitan area: land use change implications. *Remote Sens Environ*, 8 (3): 185.

[29] Hu, X., Zhou, W., Qian, Y. and Yu W. (2017). Urban expansion and local landcover change both significantly contribute to urban warming, but their relative importance changes over time. *Landsc Ecol*, vol. 32, pp. 763–780.

[30] Wilker, E. H., Yeh, G., Wellenius, G. A., Davis, R. B., Phillips, R. S. and Mittleman, M. A. (2012). Ambient temperature and biomarkers of heart failure: a repeated measures analysis. *Environ Health Perspect*, 120 (8) 1083-7.

[31] Crimmins, A., Balbus, J., Gamble, J. L., Beard, C. B., Bell, J. E., Dodgen, D., Eisen, R. J., Fann, N., Hawkins, M. D., Herring, S. C., Jantarasami, L., Mills, D. M., Saha, S., Sarofim, M. C., Trtanj, J. and Ziska L. (2016). *Impacts of Climate Change on Human Health in the United States*: A Scientific Assessment. U. S Global Change Research Program, Washington, DC, 312 pp. dx.doi.org/10.7930/J0R49NQX.

[32] Patz, J., Lendrum, D. C., Holloway, T. and Foley J. (2005). Impact of regional climate change on human health. *Nature*, vol. 438, pp. 310–317.

[33] Ropo, O. I., Perez, M. S., Werner, N. and Enoch, T. I. (2017). Climate variability and heat stress index have increasing potential III-health and environmental impacts in the East London, South Africa. *Int J Appl Eng Res*, 12 (17) 6910–6918.

[34] Oke T. R. (1978). *Boundary layer climates*. Methuen & Co., London.

[35] Shuttleworth W. J. (2012). *Terrestrial Hydrometeorology*. First edition, published by John Wisel & Sons, Ltd, pp. 51–63.

[36] Environmental Protection Agency (2010). *Methane and Nitrous Oxide Emissions from Natural Sources. Washington*, DC: US Environmental Protection Agency.

[37] Spickett, J. T., Brown, H. L. and Rumchev K. (2011). Climate change and air quality: the potential impact on health. *Asia Pac J Public Health*, 23 (2): 37S–45.

[38] Olabode Abiodun Daniel (2015). Urban Extreme Weather: A Challenge for a Healthy Living Environment in Akure, Ondo State, Nigeria. *Climate*, vol. 3, pp. 775–791. doi: 10.3390/cli3040775.